

UDK 622.785:691.54

Quantitative Formulation of Mechanism of Sintering Process during Creep Deformation of Refractory Concretes

A. Terzić^{*)}, Lj. Pavlović

Institute for Technology of Nuclear and other Raw Mineral Materials, Franchet d'Esperay 76, Belgrade, Serbia

Abstract:

This paper is concerned with quantitative formulation of the mechanism of the sintering process during secondary state creep deformation of refractory concretes. Investigated concretes varied in, both, chemical and mineralogical compositions. The sintering process during secondary state creep within refractory concrete has an isothermal character. Thus, an attempt was made to describe the mentioned process quantitatively. Creep was investigated at three different temperatures: 1200, 1300 and 1400°C. Variations of the microstructure of concrete samples, exposed to constant static pressure and constant temperature during certain time-intervals, were investigated using a scanning electron microscope. Obtained results of the investigation proved that creep resistance is an irreplaceable method when the decision about the best possible type of refractory concrete for application in metallurgical furnaces is required.

Keywords: *Creep, Sintering, Refractory concrete, Microstructure*

1. Introduction

The use of refractory concretes, as an unshaped refractory material, in monolithic elements of metallurgical furnaces and other plants operating at high temperatures is, today, irreplaceable. Production of calcium aluminate cement (CAC), which commenced at the beginning of the 20th century, initiated manufacturing of refractory concretes. During the late 70's, a new trend in manufacturing of refractory concretes appeared. Namely, this period was marked with the development of a new type of concrete: low-cement refractory concrete. The aim of the mentioned research was to find the best possible composition for refractory concretes with a low content of CaO and by that to obtain properties such as high refractoriness, good corrosion resistance and high creep resistance. A lower content of calcium aluminate cement affects the necessity of concrete for water (decreases it) to enable hydraulic bonds and decreases the level of porosity after drying. Creep resistance is, by no means, one of the most important thermo-mechanical properties of refractory concretes [1,2].

According to the scientific definition, creep is a plastic deformation which is a time-dependent function of a material at constant temperature and constant stress (here 0.2 MPa). In ceramic materials, creep normally takes place at temperatures above $0.5 \cdot T_m$ (where T_m is the melting temperature of the material). Creep tests (also called creep resistance tests) can be

^{*)} Corresponding author: anja.terzic@gmail.com

carried out in tensile, compressive and bending modes. However, creep is generally investigated in compressive mode, although tensile creep is faster for the same temperature and applied load.

There are three stages within the creep curve: primary, secondary (steady) and tertiary creep. Secondary state creep is the dominating region in the creep curve and constitutes the longest part of the "life" of the material in actual service. Namely, a material, which is deforming by creep, spends the longest period of time in the secondary state region of creep. [3, 4]

Secondary state creep can be described with the following equation: [4]

$$\varepsilon_s = A \cdot (D \cdot G \cdot b / K \cdot T) \cdot (b/d)^p \cdot (\sigma/G) \cdot \sigma^r \quad (1)$$

Where:

D - appropriate diffusion coefficient;

G - shear modulus of ceramics at test temperature;

b - Burgers vector;
size;

K - Boltzmann's constant;

T - temperature in Kelvin;

The diffusion coefficient (D) is given by:

$$D = D_0 \cdot \exp(-\Delta H/RT) \quad (2)$$

Where:

D_0 - frequency coefficient;

ΔH - activation energy of the creep process;

R - gas constant.

Equation (1) and (2) can be combined in order to give following equation:

$$\varepsilon_s = A_0 \cdot \sigma^r \exp(-\Delta H/RT) \quad (3)$$

Where:

A_0 - constant;

ε_s - rate of creep process.

Equation (3) is power law creep and it is the most popular law in numerous applications (for example in the cases of refractory concretes and other ceramic materials).

Two different types of creep mechanisms are possible: dislocation creep and diffusion creep. The first type is dependent on the movement of dislocations and the other on the flow of vacancies. If the rate of creep is controlled by dislocation mechanisms, the creep process occurs within the grain. In such a case the diffusion coefficient from equation (1) relates to lattice diffusion which is, in return, controlled by the slowest movement of ions. In the case of refractory concretes, diffusion creep mechanisms can be explained as follows: the diffusion of atoms takes place from grain boundaries towards other grain boundaries, whereas its path is almost parallel to the tensile axis or almost perpendicular to the tensile axis (depending on whether process of lattice and/or boundary diffusion creep is controlled by anions or by cations). Finally, the rate of diffusion creep is determined by the rate of movement of the slowest diffusion particles along its fastest diffusion path [5].

Beside temperature and stress, the creep resistance of refractory concretes is affected by the porosity of the material and its average grain size.

Thus, the general conclusion is that compressive creep is affected by the chemical and mineralogical compositions of the refractory concrete, by the temperature of firing of samples, and by the texture and the microstructure of the material [6,7].

The following equation describes assumed relationship between x (value which describes a property of the used material which varies during the sintering process) and t (duration of the sintering process). This equation is a quantitative description of sintering of refractory concrete during secondary state creep under the form of an exponential function:

$$x = k \cdot t^n \quad (4)$$

Where:

x - a property of the material that is variable during the process of sintering;
 t - duration of the process of isothermal sintering during secondary creep state;
 k - time constant;
 n - time exponent.

In the case of an investigation of the mechanism of the sintering process, using the variable of dimensional change (linear shrinkage), Pines' equation of sintering can be applied for quantitative data processing [10]:

$$\Delta l/l_0 = k \cdot t^n \quad (5)$$

The time exponent can be calculated using equation (6) during secondary state creep because temperature is constant:

$$n = \log(t_2 \cdot (\Delta l/l_0)_{T1}) / (t_1 \cdot (\Delta l/l_0)_{T2}) \quad (6)$$

Where:

t_2 and t_1 are the durations of the isothermal processes of sintering which occur in secondary state creep;

$(\Delta l/l_0)_{T1}$ and $(\Delta l/l_0)_{T2}$ are the relative dimensional changes of samples which occur at temperatures T_1 and T_2 .

The activation energy for the sintering process can be calculated using the following equation:

$$E = (R \cdot T_1 \cdot T_2 / (T_1 - T_2)) \cdot \ln(v_1/v_2) \quad (7)$$

Where:

E - activation energy;

v - rate of sintering process ($V = \Delta l / \Delta t$);

Δl - shrinkage of a sample;

Δt - duration of shrinkage process.

For calculating the activation energy of the sintering process, besides equation (7) suggested by German [9], another equation derived from Frenkel's model of sintering [9] can be used:

$$\Delta l / l_0 = (\sigma \cdot t) / (2 \cdot r \cdot \eta) \quad (8)$$

Where:

σ - specific surface energy of boundary grains at the contact;

r - diameter of grains (particles);

η - viscosity.

$$\eta = A \exp(-E/RT) \quad (9)$$

Where:

E - activation energy of the sintering process (case of viscous flow);

T - temperature of sintering process.

Thus, the final form of the equation (8) would be:

$$\Delta l / l_0 = k \cdot T^2 \cdot \exp(-E/RT) \quad (10)$$

If equation (10) is to be transformed into its logarithmic form, activation energy of the sintering process could be calculated from the diagram of $\log(\Delta l/l_0) \cdot (1/T^2)$ and $1/T$ dependence, as the coefficient of the slope of the curve.

2. Experimental

Creep tests of two different types of concretes, containing different volume fractions and types of refractory aggregates, was carried out. B type concrete containing bauxite, and K type concrete containing corundum as aggregates were investigated. Aggregates had different granulations. Both types of concrete were prepared with SECAR 70 high aluminate cement.

Samples prepared for the creep tests were of cylindrical shape. Dimensions were 50mm x 50mm. A hole was drilled in the center of each sample and its diameter was 5mm. Samples were shaped by pouring green concrete mixture into special testing moulds.

Afterwards, they were cured at the room temperature (25°C) and left in a special climate chamber for the following 24 hours. After curing, samples were extracted from the moulds and then dried at 110°C. Samples were then pre-fired at 1100°C. Sample surfaces were polished using diamond paste. A compressive creep apparatus (Netzsch, Germany) was used in the creep investigation. Pre-fired samples were heated at a rate of 5°C/min from room temperature up to the testing temperature (1200, 1300 or 1400°C) in the compressive creep apparatus. During investigation, samples were submitted to a constant compressive static load (0.2 MPa) at temperatures of 1200, 1300 and 1400°C, respectively, for 30 hours each. During this period secondary (steady) state creep was reached. Investigation was performed according to JUS standards.

3. Results and discussion

The chemical compositions of the investigated concretes are presented in Tab. I.

Tab. I Chemical composition of the concrete types VB/B and VB/K

oxide	content, (%)	
	bauxite based concrete, VB/B	corundum based concrete, VB/K
Al ₂ O ₃	62,88	93,62
SiO ₂	21,17	0,07
CaO	8,26	5,97
MgO	0,35	0,03
Fe ₂ O ₃	1,57	0,066
Na ₂ O	0,059	0,21
K ₂ O	0,56	-
TiO ₂	2,03	0,007
LI	2,58	0,12

For investigating the mechanical properties of refractory concretes, samples were cast and shaped, and afterwards thermally treated in accordance with actual, valid standards. Results of the investigation of the physical, mechanical and thermal properties are presented in Tab. II.

Tab. II Physical, mechanical and thermal properties of investigated refractory concretes

parameter	type of refractory concrete	
	VB/B	VB/K
bulk density, (g/cm ³) *	2,03	2,46
water absorption, (%) *	15,2	10,1
refractoriness	20 SK / 1540°C	34 SK / 1755°C
refractoriness under load (0,2 MPa)		
- Ta, (°C)	1300	1500
- Te, (°C)	1570	>1600
mechanical pressure strength, (MPa)*	16,9	25,3
apparent porosity, (%) *	33,2	27,1

This investigation was primarily concerned with basic creep curves on which power law creep was applied. Calculation of parameters such as the stress exponent and activation

energy was also performed. Time dependence of viscoplastic deformation of the material, at constant temperature and constant load (0.2 MPa), was investigated for both types of refractory concretes, bauxite and corundum based ones. Creep results are presented in Tab. III.

Tab. III Creep deformation of refractory concretes VB/B and VB/K

	type of refractory concrete		type of refractory concrete		type of refractory concrete	
	VB/B	VB/K	VB/B	VB/K	VB/B	VB/K
time	ε , deformation at 1200°C		ε , deformation at 1300°C		ε , deformation at 1400°C	
after 5 hours	-1,86	-2,25	-3,10	-3,24	-4,28	-4,17
after 30 hours	-2,57	-2,94	-3,60	-3,72	-4,6	-4,48
$\Delta\varepsilon$, %	-0,71	-0,69	-0,5	-0,48	-0,32	-0,31

Creep curves obtained for both refractory concretes (VB/B and VB/K) are given Fig. 1 and 2.

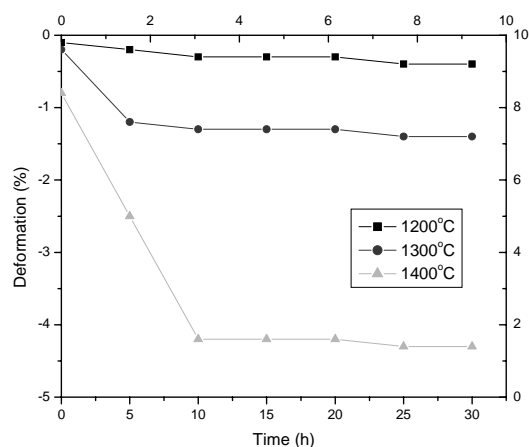


Fig 1. Creep curve for VB/B

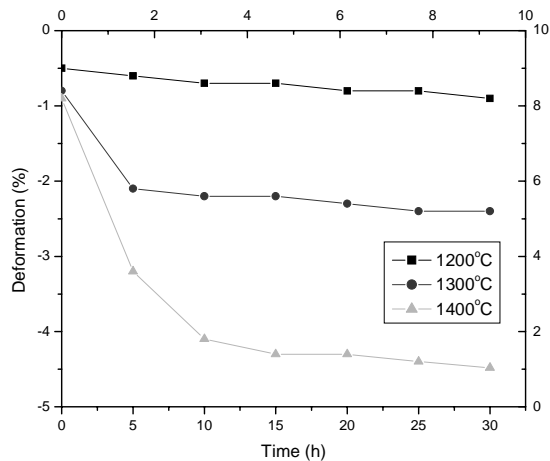


Fig 2. Creep curve for VB/K

As it has been previously noted, the viscoplastic deformation (creep) curve, generally, consists of primary, secondary (steady state) and tertiary creep. In most "engineering" materials, such as refractory concretes, investigation of the secondary state creep is of prime importance, although it can last for a long period of time. Analysis of the creep curves of refractory concretes VB/B and VB/K, presented in Fig. 1 and 2, shows that maximal deformations occur at the temperature of 1400°C. They are 4.6 and 4.48 % respectively. The percentage of the compressive creep deformation of refractory concretes increases with rising temperature. The shapes of the curves are almost similar at all three applied temperatures.

Primary creep lasts for round 5 hours for both concrete types. Transition from primary to secondary state creep is hardly noticeable at 1200°C. On the other hand, the transitions at 1300 and 1400°C are clearly visible. Onset of tertiary state creep was not detected due to the short interval of investigation (30 hours).

The fine matrix, which is situated in inter-aggregate space within concrete, is changing with increasing temperature and, above 1200°C, its viscosity diminishes significantly. Thus, plastic deformation of concrete measured at 1400°C was higher than deformation at 1200 and 1300°C for both types of concretes. It was due to the formation of a relatively high amount of liquid phase from which secondary mullite crystallizes. Newly

formed mullite increases the resistance to deformation at high temperature. The amount of mullite depends on Al_2O_3 - SiO_2 ratio.

The creep deformation of the refractory concrete at 1400°C is higher than creep deformation at 1200 and 1300°C due to surplus of the liquid phase. 90% of the deformation has already taken place at 1400°C. In the following interval, the rate of deformation changed significantly and, after that, very little deformation was observed. Initial deformation is facilitated by an insufficient amount of mullite in the microstructure, whose formation requires a significant time, when at the highest test temperature. Mullite formation induces a structural reinforcement that causes more rapid mechanical hardening of concrete at higher temperatures.

3.1 Quantitative formulation of the mechanism of the sintering process during secondary state creep

The sintering process during secondary state creep has been investigated using results of dimensional change of two different types of refractory concretes (VB/B and VB/K) obtained during the creep test. Using equations (4), (5), (6), (7) and (8) approximate coefficients of reaction mechanism and activation energy were calculated.

The durations of the dimensional change (shrinkage) of concrete samples were measured and afterwards used in the calculation. Dimensional change (shrinkage) was registered on paper by an automatic writer for each time interval.

Tab. IV Approximate rate of sintering during creep and coefficient of mechanism of reaction for VB/B

T(°C)	n	V x 10 ⁻³ (mm/min)	mechanism of reaction
1200	0,21	0,53	surfacial diffusion
1300	0,34	0,63	diffusion along the grain boundary
1400	0,52	0,92	plastic-viscous flow

Tab. V Approximate rate of sintering during creep and coefficient of mechanism of reaction for VB/K

T(°C)	n	V x 10 ⁻³ (mm/min)	mechanism of reaction
1200	0,13	0,62	surfacial diffusion
1300	0,28	0,76	surfacial diffusion
1400	0,39	1,02	diffusion along the grain boundary

Tab. IV and V show numeric results for the coefficient of reaction mechanism of the sintering process and the rate of sintering for concretes VB/B and VB/K at 1200, 1300 and

1400°C. The sintering rates and temperature dependences were calculated using the coefficient of direction (slope) of the function $\Delta L = f(\Delta t)$.

The coefficient n , which is characteristic of the reaction mechanism, has been calculated for both types of concrete, i.e. the mechanism of particle transport during sintering process in secondary state creep. From Tab. IV and V it can be seen that the most dominant mechanisms are: surface diffusion, diffusion along grain boundary and plastic-viscous flow for bauxite based concrete at temperatures 1200, 1300 and 1400°C respectively; and mechanism of surface diffusion at 1200 and 1300°C and diffusion along grain boundaries at 1400°C for corundum based concrete.

Tab. VI Approximate activation energy for VB/B and VB/K

T (°C)	temperature 1300°C	
	VB/B	VB/K
1200-1300	89,2	84,5
1300-1400	76,9	82,1

Obtained results for activation energy of sintering process during secondary state creep are approximate values.

3.2 Investigation of microstructure

3.2.1 Microstructure before creep investigation

The microstructures of concretes were examined using scanning electron microscopy. SEM (SEM JEOL JSM-5300) photomicrographs of refractory concrete samples, heat treated at 1100°C, are shown in Fig. 3 and 4. Refractory concretes have heterogeneous microstructure. Aggregate particles several millimeters in size can be seen surrounded with a fine matrix composed of micronic sized particles. Also, pores of various sizes can be seen. Porosity of these samples was calculated using Image Pro Plus, a computer program for image analysis. The calculated porosity is 33.2 and 27.1 % for bauxite and corundum concretes respectively, measured at room temperature after thermal treatment at 1100°C.

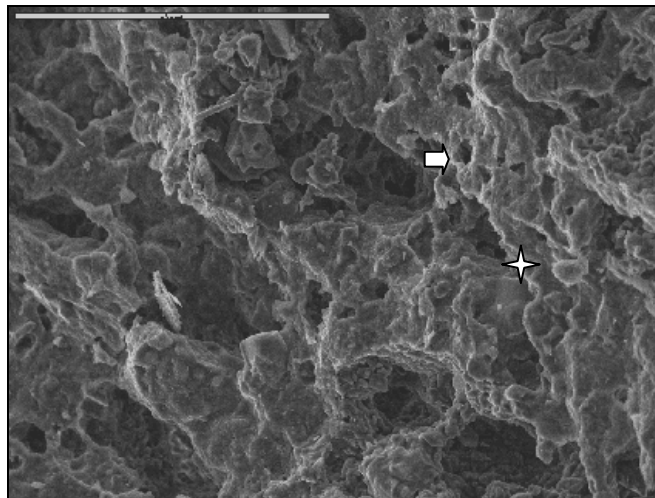


Fig 3. SEM of bauxite based refractory concrete previously heat treated at 1100°C (the arrow is pointing to a pore, and the star to the grain surrounded by matrix)

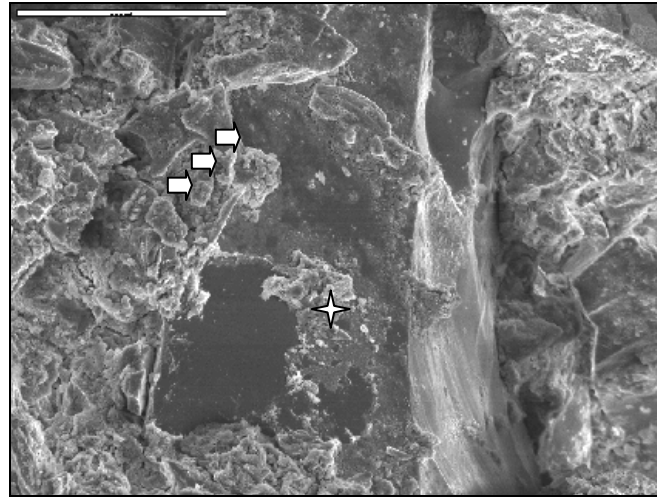


Fig 4. SEM of corundum based refractory concrete previously heat treated at 1100°C (upper arrows are pointing to pores, and the star to the large corundum grain surrounded by matrix)

3.2.2 Microstructure after creep investigation

The microstructures of samples creep tested at various temperatures are presented in Fig. 5 (a, b, c) and 6 (a, b, c). Samples fired at 1200°C (Fig. 5a and 6a) exhibit little structural change when compared to the samples heat treated at 1100°C. Structural changes start to be noticeable on the samples exposed to 1300°C. Formation of a liquid phase and emersion of initially formed crystals can be noticed. The microstructures of samples investigated at 1400°C are significantly different than the microstructure of the rest of the samples. Formation of mullite is noticed in the structure. Mullite provides structural reinforcement and makes the creep rate slower (rate of deformation). A larger amount of secondary mullite is noticed in the sample VB/B, and can explain the smaller deformation of these samples during secondary creep, when compared with concrete VB/K. Phases analyses confirmed the presence of mullite in concrete samples. There is also a significant difference in porosity. Namely samples of bauxite concrete have a noticeably higher porosity than concrete with corundum.

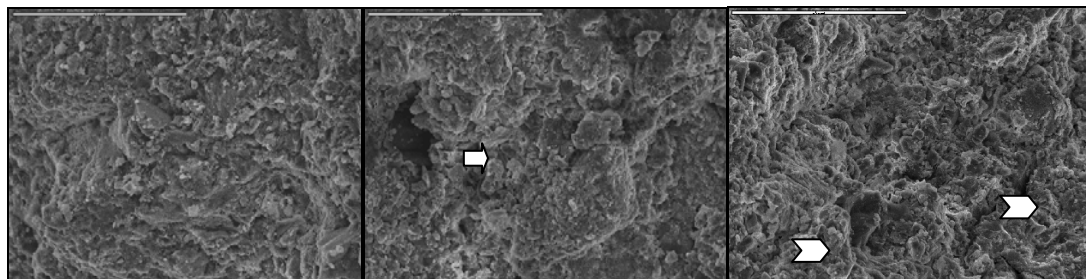


Fig. 5 SEM of bauxite based refractory concrete heat treated at a) 1200°C; b) 1300°C; c) 1400°C

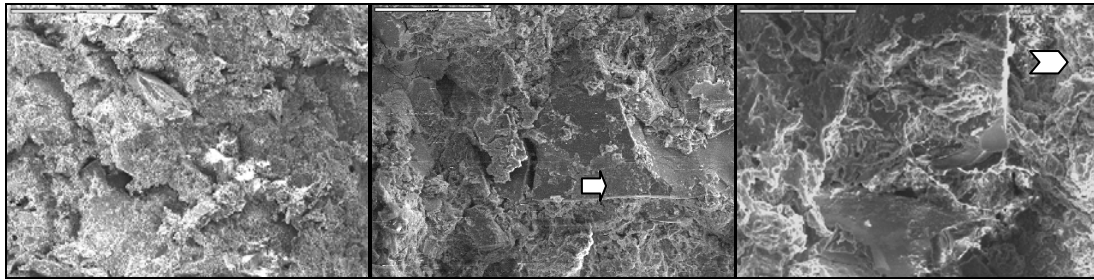


Fig 6. SEM of corundum based refractory concrete heat treated at a) 1200°C; b) 1300°C; c) 1400°C

4. Conclusion

Investigation of a time dependent viscoplastic deformation at various constant temperatures (1200, 1300 and 1400°C) and constant static load lead to the following conclusions: concrete samples investigated at 1400°C showed smaller deformation than the same samples investigated at 1200°C and 1300°C. At these temperatures the material reaches secondary state creep. This phenomenon can be explained as follows: at higher temperatures, structural reinforcement occurs due to the formation of secondary mullite situated in inter-aggregate space. This affects creep and decreases deformation.

Three different mechanisms of sintering have been spotted during the creep resistance investigation of refractory concrete samples. Those mechanisms are dependent on the applied temperatures and on chemical composition of samples. In the case of VB/B the following mechanisms were noted: surface diffusion at 1200°C, diffusion along the grain boundaries at 1300°C and plastic viscous flow at 1400°C. In case of VB/K, the following mechanisms applied: surface diffusion at 1200 and 1300°C, and diffusion along grain boundaries at 1400°C.

Approximate values of activation energy for temperature intervals 1200-1300 and 1300-1400°C are 89.2 and 76.9 kg/mol for the bauxite based concrete and 84.5 and 82.1 kg/mol for the corundum based concrete.

Investigations and obtained results confirmed that the method of creep resistance determination is irreplaceable when it comes to the decision of choice of application of refractory concrete in metallurgical furnaces and plants operating at high temperatures.

Acknowledgement

This work has been supported by Serbian Ministry of Science under project 14200115.

References

1. F.Simonin, C. Olagnon, S. Maximilien, G. Fantozzi, *J. Am. Ceram Soc.*, 83 (2000), 81
2. Bazant, M.F. Kaplan, *Concrete at High Temperatures, Material Properties and Mathematical Models*, Concrete Design and Construction Series, Longmann Group, London, 1996
3. A.Bouguerra, A. Ledhem, F. de Barquin, *Cement and Concrete Res.*, 28 (1998), 56

4. W.N. Santos, J. Eur. Ceram. Soc., 23 (2003), 1112
5. I.A. Altun, Cement and Concrete Res., 31 (2001), 1233
6. M. Bugajski, R. Schwaiger, Self-flowing Castables – a new Type of Unshaped Refractory Products, Veitsch-Radex Rundsch, Wien, 1996
7. C.Parr, E. Spreafico, T.A. Bier, A. Mathieu, Technical paper References F 97, LAFARGE Aluminates, 75782 Paris, Cedex 16, 1997
8. H. Feldborg, B. Myhre, A.M. Hundere, UNITECR '99, Berlin, Verlag Stahleisen: Dusseldorf, Germany, 1999
9. R.M. German, Sintering Theory and Practice, Wiley-Interscience Publication, New York, 1996
10. M.Prassas, J. Phalippou, J. Zarzycki, Science of Ceramic Processing, Wiley-Interscience Publication, New York, 1986

Садржај: У раду је приказано квантитативно формулисање механизма процеса синтеровања у току проучавања деформације пузањем ватросталних бетона, који се међусобно разликују по хемијском саставу и у минералошком погледу. Пузање је испитивано на три различите температуре: 1200, 1300 и 1400°C. Промена микроструктуре узорака који су били изложени константном дејству статичког оптерећења и температуре у току дужег интервала времена проучавана је помоћу скенинг електронског микроскопа. Испитивања су показала да је метода отпорности материјала на крип незамењива када се доноси закључак о примени ватросталног бетона у металуршким и термичким агрегатима.

Кључне речи: пузање, синтеровање, ватростални бетон, микроструктура
